Investigation of the dissipative structures following microseismic diffusion during hydraulic fracturing of methane-hydrate-bearing sand

Victor Nazimko[1], *Olga* Pidgurna[2*], and *Olexiy* Kusen[1]

[1]Institute for Physics of Mining Processes, Ground Control Department, 14 Sympheropolska St, 49005, Dnipro, Ukraine
[2]Higher Educational Institution “Donetsk National Technical University”, Department of Mineral Development, 2 Shybankova Ave., 85300, Pokrovsk, Ukraine

Abstract. Hydraulic fracturing is a prospective technology for methane hydrate deposit exploitation. The evolution of hydraulically stimulated fractures around the point of liquid injection is simulated. For this purpose, the FLAC3D computer model is used because of its explicit calculation cycle that imitates real physics, prevents numerical instability, and reproduces a realistic path during simulation of the nonlinear rock massif behavior. The results of the simulation provide for new findings, namely, the spatial asymmetry and synchronism violation, spatial deviation, discontinuity, and recurrence during microseismic diffusion, which follow the process of hydraulic fracturing. In addition, dissipative structures were developed due to entropy production, since gas hydrate strata are an open thermodynamic system, which transforms and dissipates the energy of the injected liquid. The process of dissipative structure evolution should be controlled to enhance the gas yield from the hydrates.

1 Introduction

Methane hydrate is deposited in permafrost regions and deep oceanic environments. The global resource of methane in the gas hydrate exceeds the other hydrocarbon reserves. Therefore, methane hydrate can play a dominant role in the global carbon cycle in the future [1]. Na et al. [2] reviewed numerous natural gas hydrate (NGH) production technologies. Thermal stimulation, depressurization, implementation of a chemical inhibitor, and CO_2-CH_4 exchange are compared. These conventional technologies have certain advantages and disadvantages [3, 4]; however, they do not satisfy economic requirements and environmental conditions. That is why specialists are searching for new innovative technologies to exploit gas hydrate deposits. Sasaki et al. [5] presented a system of hot water injection with a pair of horizontal wells to exploit the NGH. The technology of hot water cyclic steam stimulation with a single well that has been traditionally used to improve the recovery effect in a super-heavy oil reservoir [6] proved to be effective for NGH production augmentation. Other conventional in the oil industry technologies such as partial oxidation, electrical heating

*Corresponding author: olga.pidgurnaya@gmail.com

assisted by depressurization, and CO_2 swapping depressurization promised notable progress in the development of NGH deposits [7-10].

The hydraulic fracturing process (HF) has become very popular among practitioners who extract resources from hydrocarbon and hydrothermal deposits [11-13]. This technology involves a high-pressure fluid injection into geologic deep strata that creates cracks in the deep-rock formations to stimulate production from the wells. Recently, HF has been successfully introduced for the NGH production stimulation [14]. Konno et. al [15] investigated HF as a well stimulation method during gas recovery from gas hydrate reservoirs. They injected distillate water into methane-hydrate-bearing sand, which was in a three-dimensional confining stress state. Pore pressure has increased rapidly**,** but suddenly dropped due to the delamination of the tested volume. Hydraulically stimulated fractures are developed under the action of tensile stress. The permeability of the stimulated volume increased after fracturing and was maintained even after re-confining and closing the fractures. This indicated that HF is a promising method for the well stimulation of the low-permeable gas hydrate reservoirs.

However, requirements claimed for the stimulation of a NGH deposit are much stricter than for the activation of other unconventional gases. The methane-hydrate-bearing strata should be stimulated more uniformly to activate the process of dissociation. On the other hand, discrete fracture networks (DFN) evolve mostly stochastically and are almost not amenable to control. Is it possible to produce uniform fracturing of a body, which was stimulated by HF? Can the HF process be effectively controlled? We try to answer these questions in this paper.

2 Mathematical representation and description of using the airflow energy

Computer models are the best tool to investigate new geomechanical processes greatly augmenting the development of modern rock mechanics. Jing [16] classified existent geomechanical models to finite element, boundary element, finite difference, and discrete element methods. Lei et al. [17] discussed the state-of-the-art on the use of discrete fracture networks (DFN), which are relevant for modeling structural characteristics, geomechanical evolution, and hydro-mechanical behavior of stochastically generated fracture networks in a rock mass. However, the stochastic nature of DFN introduces uncertainty to fracture distribution and evolution. Consequently, DFN models can hide important fracture features. To achieve the goal, the FLAC3D model was chosen, which can simulate an irreversible behavior of the rock mass stimulated by HF [18, 19]. FLAC3D simulates flow in parallel with the mechanical modeling, in order to capture the effects of fluid/solid interaction.

HF generates microseismicity characterized by a seismic moment [20], which is defined by the equation:

$$M = G \cdot A \cdot D, \tag{1}$$

where G – the shear modulus of the rocks involved in the micro-earthquake, Pa; A – the area of the rupture along the fracture, produced by HF, m^2; D – the average slip or displacement offset between the two sides of the fracture, m.

The seismic moment has an energy dimension, and transforming the formula, we use the incremental deformation of the volume of the rock surrounding the crack:

$$M_i = Mod_i \cdot V \cdot \Delta S_i, \tag{2}$$

where Mod – the bulk or shear moduli of the rock mass, Pa; V – the volume of the fracture, m^3; ΔS – a strain increment (dimensionless) due to fracture emergence.

FLAC3D cannot simulate a set of fractures explicitly. Thus, we may simplify Formula (2) by eliminating the factor *V*. Let us consider this expression as a specific indicator of seismic activity or specific seismic moment, namely total seismic moment divided by volume of the zone where the incremental strain was calculated by FLAC3D.

The process of fracture initiation is simulated using Hubbert and Willis formula [21]:

$$P_b = \frac{3\sigma_h - \sigma_H + T - 2\eta p_o}{2(1-\eta)}, \quad (3)$$

where P_b – breakdown pressure; σ_h and σ_H – minimum and maximum horizontal in-situ stresses, respectively; T – the tensile strength of a rock layer; p_o – the pore pressure; η – the poroelastic parameter that varies in the range of 0 to 0.5.

Recalculated permeability of the rock volume after fracture generation according to recommendations of Min et al. [22] reads:

$$k_1' = k_1\left(1 + f_{norm}\left(\Delta S_1\right)^3 + f_{\tan}\left(\Delta S_{12} + \Delta S_{13}\right)\right), \quad (4)$$

where k_1 and k_1' – permeability along direction 1 before and after HF; ΔS_1 – the normal component of strain increment; ΔS_{12} and ΔS_{13} – shear components of strain increments in planes 12 and 13; f_{norm} and f_{tan} – empirical coefficients 0.83 and 0.095, respectively.

The other components of orthotropic permeability k_2 and k_3 were recalculated replacing corresponding indexes.

3 Results and discussion

Initial data. Boundary conditions. Fig. 1 depicts a model of methane-hydrate-bearing rock strata where black lines show the grid discretized the model. The interior fragment of the model was removed for the best visibility. Dimensions of the model along axis *X* and *Z* were 300 m. Top and bottom of the model were at the distance of *Y* = 450 and *Y* = 300 m from the origin where fluid was pumped to produce HF.

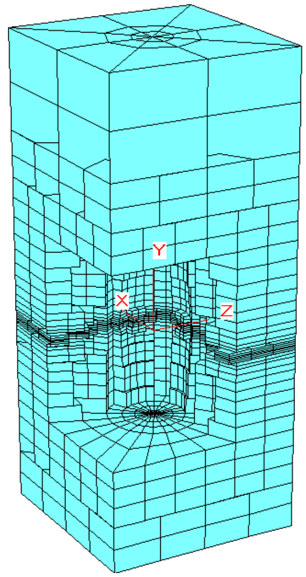

Fig. 1. FLAC3D model of the gas hydrate strata.

The model was divided into 9456 zones containing 12829 grid nodes. The geometry of the model was symmetrical relatively all axis. The displacements that are normal to lateral walls were fixed. All components of displacements were prescribed to zero on the bottom. The initial stress state in the model corresponded to the depth of 800 m at the level of the liquid injection: components of the geostatic stress σ_y, σ_x, and σ_z were 20, 10, and 10 MPa respectively in the point of injection.

Orthotropic rock mass had three basic fracture systems, namely two sub-vertical cleavages and one sub-horizontal lamination of sedimentary rocks [23]. Axial symmetry divided the model into two mirror symmetries, relatively horizontal or *X*- and *Z*-axis. It does mean that the hydraulic fractures were expected to expand synchronously in time and symmetrically in space relatively the corresponding horizontal axes, thereat along the *X*-axis quicker because permeability k_x was five times more than k_z. Mechanic and hydraulic properties of gas hydrate-bearing strata are depicted in Tables 1 and 2.

Table 1. Initial data. Mechanical properties of the rock mass.

Normal module, Pa			Shear module, Pa			Poisson ratio			Tensilte limit, MPa	Density, kg/m^3
E_1	E_2	E_3	G_1	G_2	G_3	nu_1	nu_2	nu_3	T	
$4 \cdot 10^8$	$4 \cdot 10^8$	$2 \cdot 10^8$	$1.6 \cdot 10^8$	$1.6 \cdot 10^8$	$0.8 \cdot 10^8$	0.25	0.25	0.25	$1.5 \cdot 10^5$	2500

Table 2. Hydraulic properties.

Permeability, m/s			Pore pressure, Pa	Fluid bulk modulus, Pa	Porosity	Rate of mud pumping, m^3/s	Bio coefficient
$k_1=k_y$	$k_2=k_z$	$k_3=k_x$	pp	f_{mod}	Por	v_{well}	
$1 \cdot 10^{-7}$	$2 \cdot 10^{-8}$	$1 \cdot 10^{-7}$	$3 \cdot 10^6$	$5 \cdot 10^7$	0.1	0.15	1.0

The liquid is injected under a constant rate.

Results of computer simulation. Cundall and Strack [24] proposed an explicit calculation cycle (ECC). The calculation of motion (Newton's second law) was solved ahead of the constitutive equation (stress-strain relation, including nonlinear behavior of the rock). This approach imitated real physics because the velocity of a disturbing wave is always limited in solid and liquid. Such a tactic has provided success in preventing numerical instability and reproducing a realistic path during simulation of nonlinear behavior of the rock mass. Furthermore, ECC approach provided accounting for the path of loading what is a fundamental feature of the irreversible processes [25].

ECC delivered essentially new results concerning the irreversible behavior of the fractured rock mass. These results are summarized in the following.

Spatial asymmetry and synchronism violation. Let us recall, there were both physical and geometrical symmetries in the model relatively axis *X* and *Z*, and the liquid was injected at a constant rate. Therefore, expansion of the fractured body was expected synchronously and symmetrically in space but it was not so.

Fig. 2 depicts a set of consecutive states of the fractured bodies around the coordinate origin where fluid was injected. Every state is marked with a number of cycles beginning from the start of the injection. Ten cycles correspond approximately one minute in situ. Generally, a symmetric development of the fractured body is evident but there is a tangible deviation from the symmetry. For example, set 1 residing at the positive half of the *X*-axis on the 130th cycle of injection encompassed more fractured zones than antagonistic set 2 located at the negative part of this axis. The same situation concerns the sets 3 and 4 on the 140th cycle: set 3, which is on the positive end of the *Z*-axis has two fractured zones against three zones at the negative end. The asymmetric evolvement of the fractured volume is steady and appears at later stages 160 (compare sets 5 and 6) and 180 (sets 7 and 8).

(a)

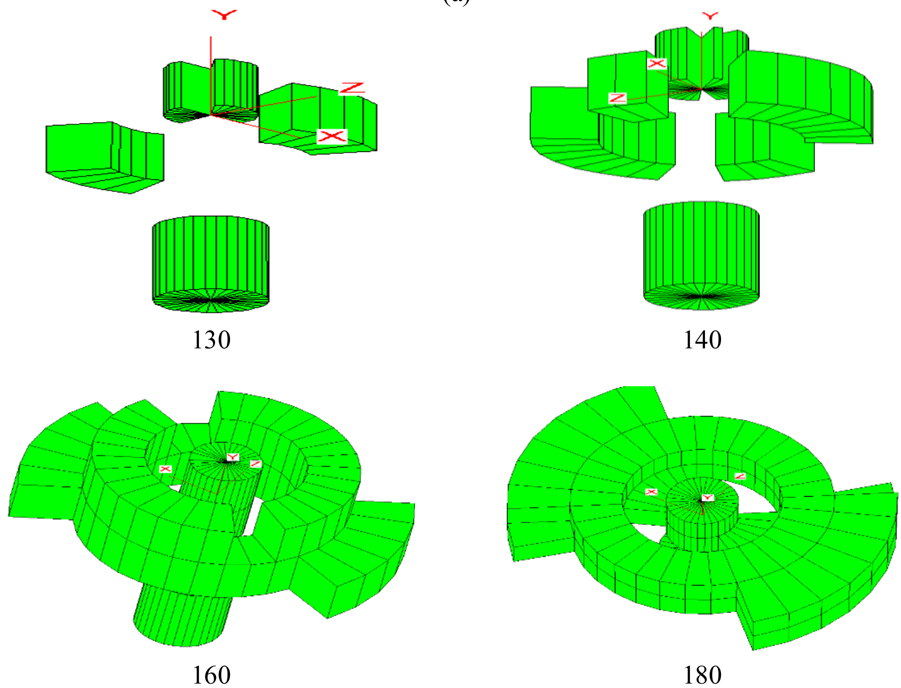

(b)

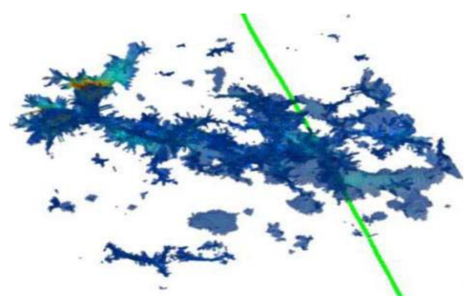

Fig. 2. Evolution of fractured body during HF deployment; numbers below the fragments indicate time of the liquid injection: A – the final shape of the fractured volume; B – results of the microseismic monitoring according to [26].

The rate of the spatial asymmetry is not big and keeps in the range of 10% but it is much more than the error of calculation that was less than $1 \cdot 10^{-5}$.

Spatial deviation, discontinuity, recurrence. Fig. 2 demonstrates that the fractured body evolution is discontinuing and discrete in space. There are blanks in the 3D fractured body where fractures are absent at the initial stage of HF process and patches of the virgin intact rock remain a long time. Geophysical monitoring of the microseismicity following HF process proved that the discrete pattern of hydraulic fracture development is a usual and natural phenomenon [26] (Fig. 2, bottom fragment).

Eventually, HF process returned to the blanked spots and disintegrated them emphasizing the recurrence of HF. It does mean the gas hydrate strata can disintegrate by turn, with separate portions in space and in time.

As a contrast, the pore pressure diffused and expanded continuously what Fig. 3 demonstrates. The shape of the pore pressure cloud tends to correspond to the permeability anisotropy because the dimensions of the cloud in the horizontal plane intersecting the point of injection relate as 1:3 that is approximately reversely proportional to the ratio of the permeability along *Z*- and *X*-axis.

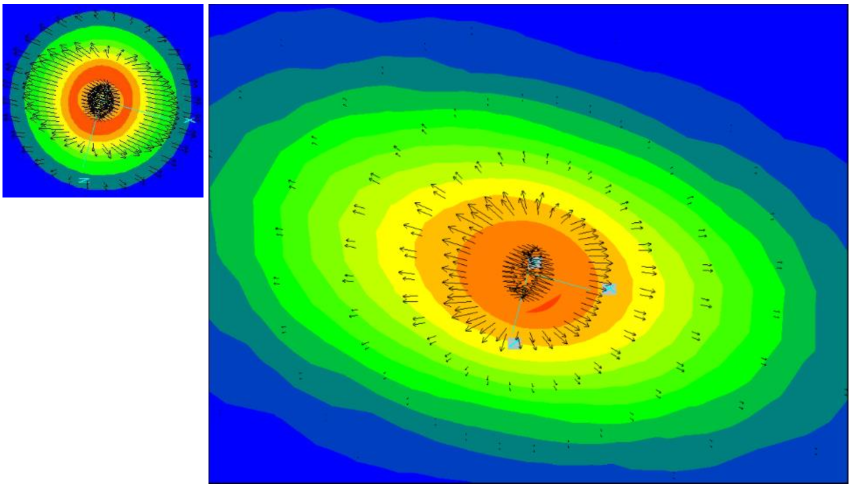

Fig. 3. Evolution of the pore pressure distribution in the horizontal plane, which goes through the point of liquid.

Dissipative structures development. Specialists in microseismicity use a diagram in coordinate "distance from the injection point" – "time" to characterize the process of microseismicity diffusion (Fig. 4). Fragment (a) demonstrates this diagram with a wireframe surface, whereas fragment (c) shows the distribution of seismic moments for a section along the horizontal plane going through the point of injection. Apparently, HF process went spontaneously to the self-organization state. Despite the uniform distribution of mechanic and hydraulic parameters of the gas hydrate-bearing strata, the microseismic intensity evolved to the complex structure in time and space.

Periodic maximums of microseismicity (indicated with white arrows in fragment (a) interchanged with a less intensive manifestation of ground/liquid pressure that perfectly coincides with the results of geophysical monitoring [27] (fragment (b) in Fig. 4 – black arrows). Furthermore, both the parabolic envelope and the boundary of the back front match on the computer (a) and experimental (b) diagrams. Such a self-organization is natural and physically substantiated because the gas hydrate strata is a typical open thermodynamic system that transforms energy of the liquid pressure dissipating it in a form of microseismic energy, the surface energy of the hydraulically stimulated fractures, and finally heat. According to [28] such a system transits to the self-organization state if the transformed energy flow is sufficiently big.

Thermodynamics of irreversible processes has evolved over the past century, and several Nobel Prizes have marked its theoretical basis. It is important from the position of gas hydrate recovery that the rock mass is susceptible to form the dissipative structures during HS deployment even if it is geologically homogeneous and has a uniform distribution of mechanic properties. The law of the minimum entropy production [28] controls a slope of the ground promoting the development of the dissipative structures. Development of the dissipative structures is triggered by small thermodynamic fluctuations, for example, a variation of ground pressure, instability of the temperature, or deviation of rock mass strength relatively average level.

(a) (b) (c)

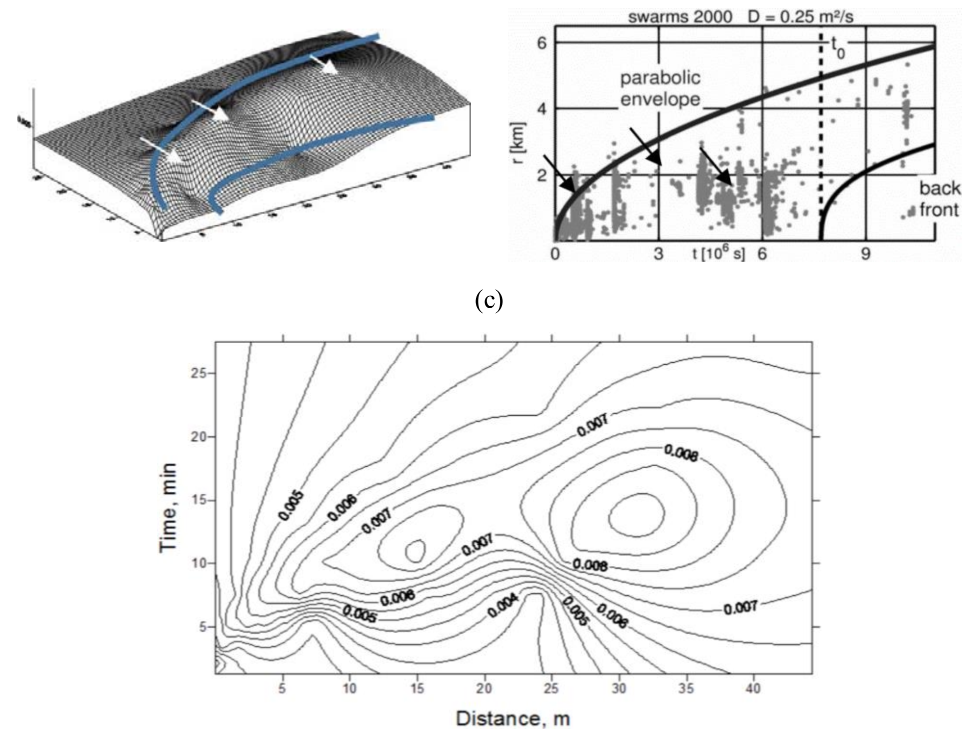

Fig. 4. Evolution of the dissipative structures: A and C – in the computer model; B – in situ according to [27].

The study showed [23] that there are natural sources of feedback that enhance the self-oscillatory process of periodic amplification and decay of HF, which is clearly shown in Fig. 4. There is a wide range of the dissipative structure patterns in a rock mass [29]: unusual irreversible ground movement sort of rotors, torrents, sinks, and sources; sequential asymmetrical expansion of disintegrated and loosening rock mass around underground opening [30]; yielding of the frame support clutches that proceeds by turn, one after another.

Computer simulation has demonstrated that HF can produce dissipative structures, which cause irregular fracturing of the gas hydrate-bearing strata. This reduces the positive effect of gas production stimulation. This disadvantage can increase because of the natural variation of the rock mass strength. Therefore, dissipative structures must be controlled and, first of all, slowed down or eliminated [23]. This is a subject for future research work.

4 Conclusions

The FLAC3D model has been used to simulate the deployment of HF in gas hydrate reservoirs at a depth of 800 m. It was found that a fractured zone around the point of liquid injection develops asymmetrically in space. This zone increases in parts and fragments one after another in different directions. The rate of spatial asymmetry is not big and keeps in the range of 10% but it is much more than the error of calculation that was less than $1 \cdot 10^{-5}$.

The fractured body evolution is discontinuing and discrete in space. There are blanks in the three-dimensional fractured body where fractures are absent at the initial stage of HF process. The patches of the virgin intact rock can remain a long time. Eventually, HF process returns to the blanked spots and disintegrates them emphasizing the recurrence of HF. At the last stage of injection, most of the blind spots were processed with HF but some intact patches could persist.

As a contrast, the pore pressure diffused and expanded continuously shaping a cloud, dimensions of which were reversely proportional to permeability in the orthotropic rock mass.

Gas hydrate-bearing strata are an open thermodynamic system, which transforms and dissipates the energy of injected liquid and ground pressure. Dissipative structures follow the HF process if the energy flow is sufficient. The dissipative structures are exposed on the two-dimensional diagram in coordinates 'distance from the injection point' – 'time' as periodic maximums of microseismicity interchanging with a less intensive manifestation of ground pressure. The inclination of the rock mass to generate the dissipative structures is governed by the minimum entropy production law. The dissipative structure development is triggered by small thermodynamic fluctuations, for example, a variation of ground pressure, instability of the temperature, or deviation of rock mass strength relatively average level.

The dissipative structures reduce the positive effect of gas production stimulation. This disadvantage can further increase because of the natural variation of the rock mass strength. Therefore, the dissipative structures should be controlled and, first of all, put a brake on or inhibited.

This work was conducted within the project "Investigation of dissipative structures and their evolution during irreversible deformation of rock mass and ground" (State registration No. 0120U100081). The authors thank Donetsksteel Company that provided key No. 024486 for simulation on FLAC3D that is highly appreciated.

References

1. Archer, D., Buffett, B., & Brovkin, V. (2008). Ocean methane hydrates as a slow tipping point in the global carbon cycle. *Proceedings of the National Academy of Sciences*, *106*(49), 20596-20601. https://doi.org/10.1073/pnas.0800885105
2. Boswell, R., & Collett, T.S. (2011). Current perspectives on gas hydrate resources. *Energy & Environmental Science*, *4*(4), 1206–1215. https://doi.org/10.1039/c0ee00203h
3. Na, S., Lei, A., Hui, D., Jian, S., Xinjun, G. (2016). Discussion on natural gas hydrate production technologies. *China Petroleum Exploration*, *21*(5).
4. Swaranjit Singh, A.A. (2015). Techniques for exploitation of gas hydrate (clathrates) an untapped resource of methane gas. *Journal of Microbial & Biochemical Technology*, *07*(02). https://doi.org/10.4172/1948-5948.1000190
5. Yang, Y., He, Y., & Zheng, Q. (2017). An analysis of the key safety technologies for natural gas hydrate exploitation. *Advances in Geo-Energy Research*, *1*(2), 100-104. https://doi.org/10.26804/ager.2017.02.05
6. Sasaki, K., Yamakawa, T., & Sugai, Y. (2014). Integrated thermal gas production from methane hydrate formation. *SPE/EAGE European Unconventional Resources Conference and Exhibition*. https://doi.org/10.2118/167780-ms
7. Li, Z., Lu, T., Tao, L., Li, B., Zhang, J., & Li, J. (2011). CO_2 and viscosity breaker assisted steam huff and puff technology for horizontal wells in a super-heavy oil reservoir. *Petroleum Exploration and Development*, *38*(5), 600-605. https://doi.org/10.1016/S1876-3804(11)60059-1
8. Godec, M., & Koperna, G. (2014). Enhanced gas recovery and CO_2 storage in gas shales: A summary review of its status and potential. *Energy Procedia*, (63), 5849-5857. https://doi.org/10.1016/j.egypro.2014.11.618

9. Cha, M., Yin, X., Kneafsey, T., Johanson, B., Alqahtani, N., Miskimins, J., & Wu, Y.-S. (2014). Cryogenic fracturing for reservoir stimulation – Laboratory studies. *Journal of Petroleum Science and Engineering*, (124), 436-450. https://doi.org/10.1016/j.petrol.2014.09.003
10. Charlez, P., Lemonnier, P., Ruffet, C., Bouteca, M.J., & Tan, C. (1996). Thermally induced fracturing: Analysis of a field case in North Sea. *European Petroleum Conference*. https://doi.org/10.2118/36916-ms
11. Chen, W., Maurel, O., Reess, T., De Ferron, A.S., La Borderie, C., Pijaudier-Cabot, G., & Jacques, A. (2012). Experimental study on an alternative oil stimulation technique for tight gas reservoirs based on dynamic shock waves generated by Pulsed Arc Electrohydraulic Discharges. *Journal of Petroleum Science and Engineering*, (88-89), 67-74. https://doi.org/10.1016/j.petrol.2012.01.009
12. Barati, R., & Liang, J.-T. (2014). A review of fracturing fluid systems used for hydraulic fracturing of oil and gas wells. *Journal of Applied Polymer Science*, *131*(16). https://doi.org/10.1002/app.40735
13. Gallegos, T.J., & Varela, B.A. (2015). Trends in hydraulic fracturing distributions and treatment fluids, additives, proppants, and water volumes applied to wells drilled in the united states from 1947 through 2010 – data analysis and comparison to the literature. *U.S. Geological Survey Scientific Investigations Report*. Reston, United States: USGS.
14. Daigle, H., Bangs, N.L., & Dugan, B. (2011). Transient hydraulic fracturing and gas release in methane hydrate settings: A case study from southern Hydrate Ridge. *Geochemistry, Geophysics, Geosystems*, *12*(12). https://doi.org/10.1029/2011gc003841
15. Konno, Y., Jin, Y., Yoneda, J., Uchiumi, T., Shinjou, K., & Nagao, J. (2016). Hydraulic fracturing in methane-hydrate-bearing sand. *RSC Advances*, *6*(77), 73148-73155. https://doi.org/10.1039/c6ra15520k
16. Jing, L. (2003). A review of techniques, advances and outstanding issues in numerical modelling for rock mechanics and rock engineering. *International Journal of Rock Mechanics & Mining Sciences*, *40*(3), 283-353. https://doi.org/10.1016/s1365-1609(03)00013-3
17. Lei, Q., Latham, J-P., & Tsang, C-F. (2017). The use of discrete fracture networks for modelling coupled geomechanical and hydrological behaviour of fractured rocks. *Computers and Geotechnics*, (85), 151-176. https://doi.org/10.1016/j.compgeo.2016.12.024
18. FLAC3D. (2008). *Fast lagrangian analysis of continua in 3 Dimensions*. Itasca Consulting Group, Inc. Version 3.10.
19. Zhou, L. (2012). 3D modeling of hydraulic fracturing in tight gas reservoirs by using of flac3d and validation through comparison with FracPro. *Advanced Materials Research*, (524-527), 1293-1299. https://doi.org/10.4028/www.scientific.net/AMR.524-527.1293
20. Aki, K., & Richards, P.G. (2002). *Quantitative seismology* (2 ed.). Sausalito, California: University Science Books.
21. Hubbert, M.K., & Willis, D.G. (1957). Mechanics of hydraulic fracturing. *Transactions of the AIME*, *210*(01), 153-168. https://doi.org/10.2118/686-g
22. Min, K.-B., Rutqvist, J., Tsang, C.-F., & Jing, L. (2004). Stress-dependent permeability of fractured rock masses: A numerical study. *International Journal of Rock Mechanics and Mining Sciences*, *41*(7), 1191-1210. https://doi.org/10.1016/j.ijrmms.2004.05.005
23. Nazimko, V.V., Saleev, I.A., Iliashov, M.O., & Zakharova, L.M. (2020). Microseismic structure evolution due to variation of liquid injection rate (07-04). *5th International Itasca Symposium*. Billaux, Hazzard, Nelson & Schöpfer (eds.). Paper: 07-04. Vienna, Austria: Itasca International, Inc., Minneapolis.
24. Cundall, P.A., & Strack, O.D.L. (1979). A discrete numerical model for granular assemblies. *Geotechnique*, 29(1), 47-65. https://doi.org/10.1680/geot.1979.29.1.47
25. Wang, J. (2009). Modern thermodynamics – New concepts based on the second law of thermodynamics. *Progress in Natural Science*, *19*(1), 125-135. https://doi.org/10.1016/j.pnsc.2008.07.002
26. Sicking, C., Vermilye, J., Geiser, P., Lacazette, A., & Thompson, L. (2013). Fracture Imaging and Permeability Fairway Mapping. *Search and Discovery Article*, 41150.

27. Parotidis, M. (2005). Evidence for triggering of the Vogtland swarms 2000 by pore pressure diffusion. *Journal of Geophysical Research*, *110*(B5). https://doi.org/10.1029/2004jb003267
28. Nicolis, G., & Prigogine, I. (1971). *Self-organization in nonequilibrium systems: From dissipative structures to order through fluctuations*. New York, United States: Wiley.
29. Nazimko, V., & Zakharova, L. (2017). Cluster behavior of the ground during its irreversible movement. *Acta geodynamica et geomaterialia*, *14*(188), 45-49.
30. Nazimko, V.V., Peng, S.S., Lapteev, A.A., Alexandrov, S.N., & Sazhnev, V.P. (1997). Damage mechanics around a tunnel due to incremental ground pressure. *International Journal of Rock Mechanics and Mining Sciences*, *34*(3-4), 222.e1-222.e14. https://doi.org/10.1016/s1365-1609(97)00245-1